Engineering Applications of Relaxation Procedures by Digital Computation

M. E. RADD and M. R. TEK

Phillips Petroleum Company, Idaho Falls, Idaho

A generalized computing method is developed to perform mathematical "relaxation" on a Datatron digital computer. The application of the developed relaxation or iteration procedures results in obtaining numerical solutions to several engineering boundary-value problems expressed by elliptic differential equations. The developed digital relaxation routine is found to be effective, fast, and practical in solving numerous steady-state heat and mass transfer problems with arbitrary and quite often complex boundary conditions. While the specific speed and accuracy of the developed digital method is found to depend upon the type of differential equation, the grid size, and computational tolerance requirements, a typical problem indicates that 250 iterations/min. speed and 1% accuracy may be achieved in an average case.

The examples presented in this paper are chosen from the more classical heat transfer and temperature and pressure distribution problems in order to indicate some other areas where similar engineering problems can be solved however complex the boundary conditions may be.

Certain types of boundary-value problems can be solved by replacing the differential equation by a finite-difference equation which is next solved by a process of iteration (*1, 2*). This method of solving partial differential equations was developed and first used by L. F. Richardson in 1910. Improvements on Richardson's original work were later introduced by Liebmann (*4*), Thom (*5*), and Shortley and Weller (*6*). A somewhat similar method is credited to Southwell (*7, 8*) and called *relaxation*. This method, quite analogous to the previous finite-difference method called *iteration*, was developed for application to problems of structural engineering (*8, 9*). An excellent comparison between iteration and relaxation methods is given in some detail by Scarborough (*2*). The application of relaxation methods to oil field research has been published by Dykstra and Parsons (*10*).

It is well known that while relaxation is rapid and liable to errors, iteration is slow, sure, but frequently long. Computational errors in the method of iteration are self-correcting; the ones likely to occur in the method of relaxation usually remain hidden. Although the choice of an appropriate method often depends on the problem to be solved, it becomes quite evident that relaxation is best suited to long-hand or desk-calculator types of computations and that iteration can readily and efficiently be performed on digital computers.

The primary objectives of this work have been to develop a generalized routine to perform this iteration on electronic digital computers and to apply this method to solve several engineering problems in areas such as heat and mass transfer, steady state fluid flow, and temperature or pressure distributions.

M. R. Tek is at the University of Michigan, Ann Arbor, Michigan.

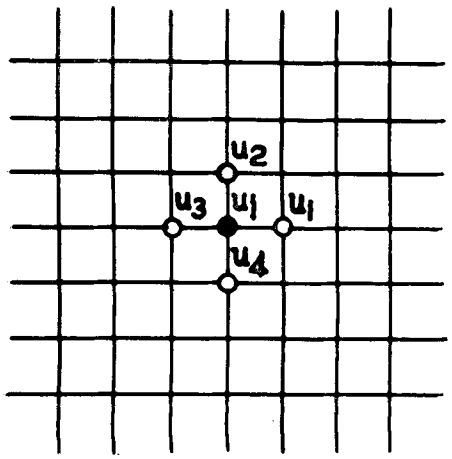

Fig. 1. Two-dimensional square grid.

ANALYSIS

Basic Differential Equations

The partial-differential equations commonly encountered in engineering problems are of second order in at least one of the dependent variables and also linear with respect to second-order derivatives. These equations are usually classified in three groups: elliptic, parabolic, and hyperbolic equations.

Elliptic Equations

$$\frac{\partial^2 u}{\partial x^2} + \frac{\partial^2 u}{\partial y^2} = a(x, y) \qquad (1)$$

Equation (1), denoting one of the most frequently used partial differential equations, is called *Poisson's equation*. A special case is obtained when $a(x, y) = 0$, and the equation is then called *Laplace's equation*:

$$\frac{\partial^2 u}{\partial x^2} + \frac{\partial^2 u}{\partial y^2} = 0 \qquad (2)$$

When the Navier-Stokes equations are written and simplified for the case of steady state, streamline, viscous pipe flow, an equation quite similar to Equation (1) is obtained:

$$\frac{\partial^2 w}{\partial x^2} + \frac{\partial^2 w}{\partial y^2} = \frac{1}{\mu}\frac{dP}{dZ} = a \qquad (3)$$

Calculations of steady state temperature distributions in heat-conduction and boundary-value problems resulting from theories of elasticity, plasticity, stress analysis, and electrostatic or electromagnetic field potentials are typical of applications of elliptic partial-differential equations.

When elliptic equations are considered, it becomes necessary to specify boundary conditions at every point of a well-defined closed boundary. Parabolic and hyperbolic equations are usually associated with a domain which is at least open in the direction of one variable, usually the time variable. The techniques and methods for the numerical solutions of parabolic and hyperbolic equations have been much less explored than those for the elliptic equations.

In this study computer solutions are developed for the elliptic equations of types 1, 2, and 3. In particular a digital solution for the case.

$$\frac{\partial^2 u}{\partial x^2} + \frac{\partial^2 u}{\partial y^2} = -fu - g \qquad (4)$$

has also been developed.

The Finite-Difference Equations

As indicated in Figure 1, when a network (x = constant, y = constant) is laid

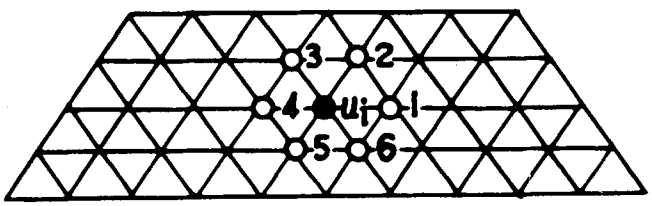

Fig. 2. Two-dimensional triangular grid.

upon a given continuum of points in two-dimensional space, the finite-difference equation corresponding to Poisson's Equation (1) is given by

$$u_i = \tfrac{1}{4}[u_1 + u_2 + u_3 + u_4 - h^2 g(x_i, y_i)] \quad (1a)$$

which can also be written as

$$u_i = \tfrac{1}{4}\sum_{j=1}^{4} u_j - \frac{h^2}{4} g(x_i, y_i) \quad (1b)$$

where h represents Δx and Δy in a square grid.

The finite-difference equation corresponding to Laplace's equation can be simply given as

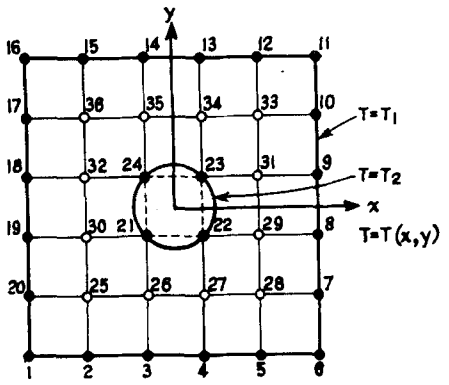

Fig. 3. Approximate network representation of a boundary-value problem.

triangular network (Figure 2) the finite difference equation corresponding to Laplace's equation is given as

$$u_i = \tfrac{1}{6}\sum_{j=1}^{6} u_j \quad (5)$$

The computer solutions developed in this report are, however, prepared for applications on square grids only.

Development of Digital Techniques

To illustrate the iterative procedure, a typical problem is presented. Figure 3 indicates the boundaries and the interior grid points of a two-dimensional model, where the distribution of a $T = T(x, y)$ function is desired. The points 1 through 20 represent the outside boundaries, and the points 21 through 24 represent the inside boundaries. The points 25 through 36 are the interior grid points at which the values of $T = T(x, y)$ are desired. T may represent the temperature function in a homogeneous solid (Figure 3), where constant temperatures are maintained at the inside and outside boundaries.

The differential equation to be satisfied is $(\partial^2 T)/(\partial x^2) + (\partial^2 T)/(\partial y^2) = 0$. The boundary conditions are $T_i = T_1 (i = 1, 2, 3, \cdots 20)$ and $T_j = T_2 (j = 21, 22, 23, 24)$. The finite-difference equation corresponding to this is

$$T_i = \tfrac{1}{4}\sum_{j=1}^{4} T_j \quad (6)$$

To start the process, rough approximations are first made on all unknown internal grid-point temperatures.

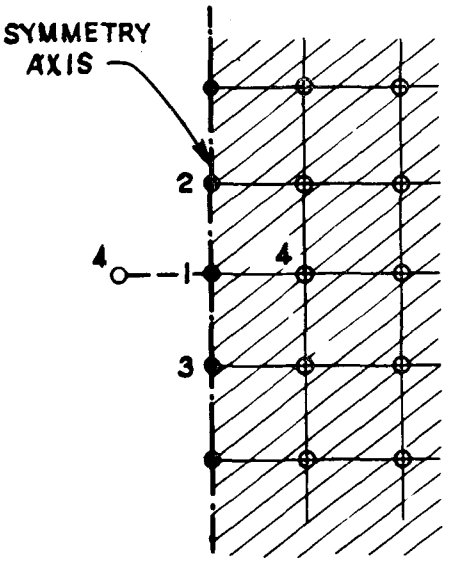

Fig. 4. Iteration at symmetry axis.

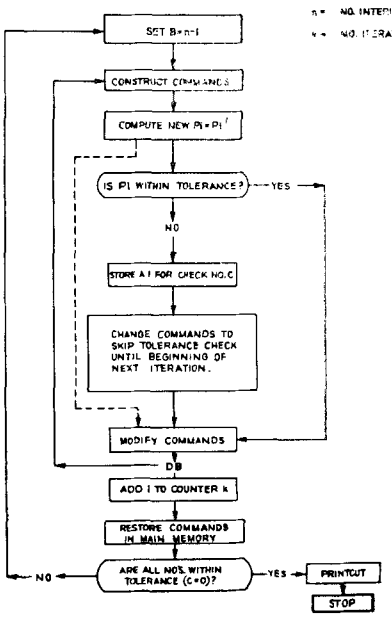

Fig. 5. Block diagram digital relaxation.

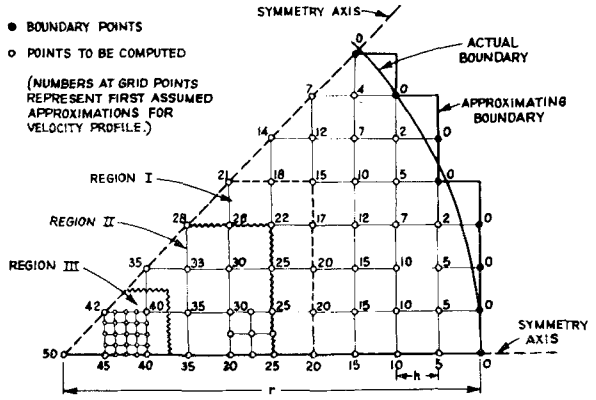

Fig. 6. Cross sectional area for pipe flow.

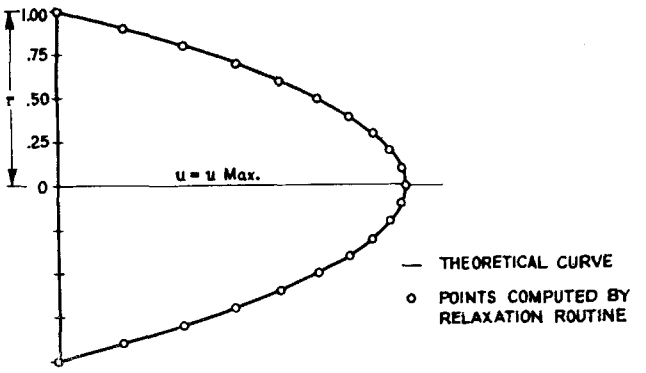

Fig. 7. The velocity profile.

$$u_i = \tfrac{1}{4}\sum_{j=1}^{4} u_j \quad (2a)$$

A similar derivation for Equation (4) gives

$$u_i = \left(\frac{1}{4 - h^2 f}\right)\sum_{j=1}^{4} u_j + \frac{h^2 g}{4 - h^2 f} \quad (4a)$$

It will be noticed that most of the examples given in this study are based on a square grid network. However this generally is not necessary. Although the square network is the simplest, a network of equilateral triangles sometimes becomes more suitable to a particular problem. In the case of an equilateral-

An example is point 25. If the superscripts refer to the order of successive approximations, the first approximation being the orginal assumed temperature, the second approximation is given by

$$T_{25}^{(2)} = \tfrac{1}{4}[T_2 + T_{26}^{(1)} + T_{30}^{(1)} + T_{20} \quad (7)$$

Next the second approximation for T_{26} is calculated in a similar manner by using the improved values of its adjacent points as soon as they are available.

Equations (6) and (7) are thus successively used at each point until such time as the modifications become in-

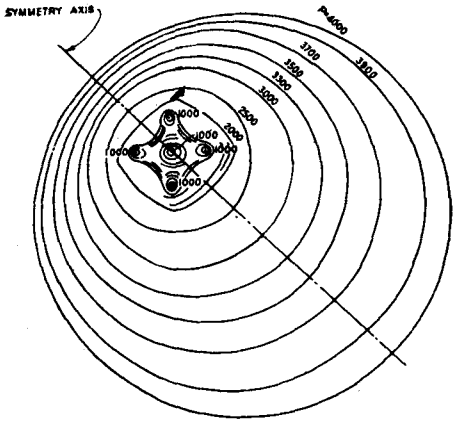

Fig. 8. Steady state pressure distribution in a reservoir.

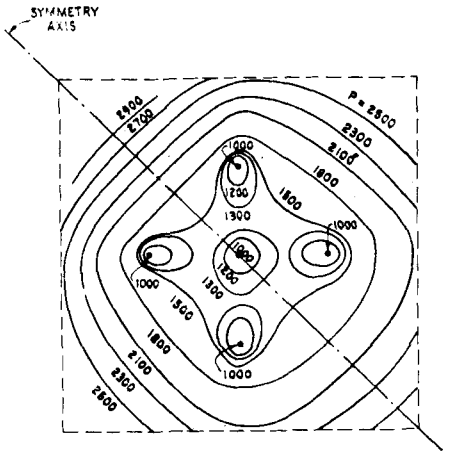

Fig. 9. Steady state pressure distribution (enlarged subregion of reservoir).

appreciable. Every step thus relieves some particular constraint due to forcing the original assumed or subsequent approximated value of the unknown function. The successive iterations are stopped only when the dependent variable becomes relaxed, that is, can no longer be further improved by repeating earlier steps.

As shown in Figure 4, whenever a certain symmetry becomes evident, the problem needs only to be solved for regions bounded by the symmetry axes. This saves a considerable amount of duplicated effort.

In the event that a point to be iterated falls on one of the symmetry axes (note Figure 4) in performing its iteration, the point off the axis of symmetry must be counted twice to include the effect of its image with respect to the axis of symmetry; that is

$$T_1 = \tfrac{1}{4}[T_2 + T_3 + 2T_4] \qquad (7a)$$

It usually is advisable to start with a coarse grid, then to repeat with a finer grid, especially in some interesting subregion of the problem.

Digital Relaxation on the Datatron

The systematic and mechanical nature of the iteration technique described suggested its programmability on a digital computer. A Datatron routine was developed and is now available to perform *relaxation by digital computation.* This routine handles as many as 1,000 interior and 800 boundary grid points. Two main memory cells are allocated to each interior grid point. The data in these cells identify the serial numbers of each considered point and the adjacent grid points. The input data as well as the program are on paper tape. The output is on the line printer.

The routine is coded, fixed-point arithmetic; therefore the true decimal-point location could be anywhere as long as all points are consistent. When the value at every computed point shows no change from the previous iteration, the line printer records the number of iterations and the answers with the corresponding index numbers. The iterations continue as long as there is at least one point that is not within a given tolerance.

Figure 5 represents the *block diagram* of the digital relaxation routine, indicating the programming logic used. The B-register is set at the beginning to $(n - 1)$. Next commands to perform the relaxation calculations are constructed and stored.

For a given point i the unknown function P_i is computed and checked. If the calculated value is within the required tolerance, the next point P_{i+1} is computed and checked; if one point is not within the tolerance, then for the remaining points during that particular iteration the tolerance checks are omitted. The number of iterations is tallied in a counter k and, when all the computed points meet the tolerance check, the answers are printed and the computer stops.

APPLICATIONS

The digital relaxation method developed during this study has been successfully applied to several engineering problems. Some of these applications were purposely chosen from heat transfer, pressure, and flow distribution problems for which theoretical solutions were readily available. These applications were quite useful as checkout tools; they also provided valuable information regarding the over-all computing time, accuracy, and reliability of the answers.

The following typical problems are given as examples of direct engineering applications to emphasize the practical

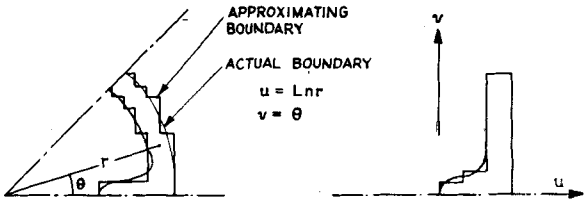

Fig. 10. Sector of internally finned tubular reactor and its conformal mapping.

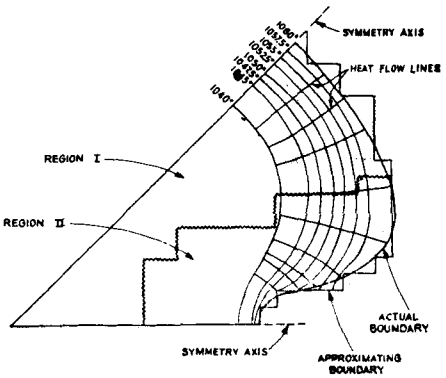

Fig. 11. Butane dehydrogenation isotherms and heat flow lines in an internally finned catalyst tube.

significance of this method in solving a large number of steady state problems. It is hoped that through these examples the reader will see some areas of application where his problems may be solved no matter how complicated the boundary conditions may be.

Pipe-Flow Velocity Distribution

The classical case of steady state (streamline) pipe flow is given as a prominent example of an elliptic boundary-value problem and as an illustration of some techniques developed for proper choice of space increments and tolerance specifications. When the Navier-Stokes equations are written for the general case and then simplifications are introduced owing to steady state, unidirectional, and incompressible flow conditions, the following equations are developed:

$$\rho \frac{Dw}{Dt} = -\frac{\partial P}{\partial Z} + \rho F_z + \mu \nabla^2 w + \tfrac{1}{3}\mu \frac{\partial \theta}{\partial Z} \qquad (8)$$

where

Dw/Dt = 0 steady-state condition
$\partial P/\partial Z$ = constant = dP/dZ, (unidirectional flow, constant-rate pressure drop)
F_z = 0 assumed
θ = 0 incompressible flow

Then

$$\nabla^2 w = \frac{1}{\mu}\frac{dP}{dZ} \qquad (9)$$

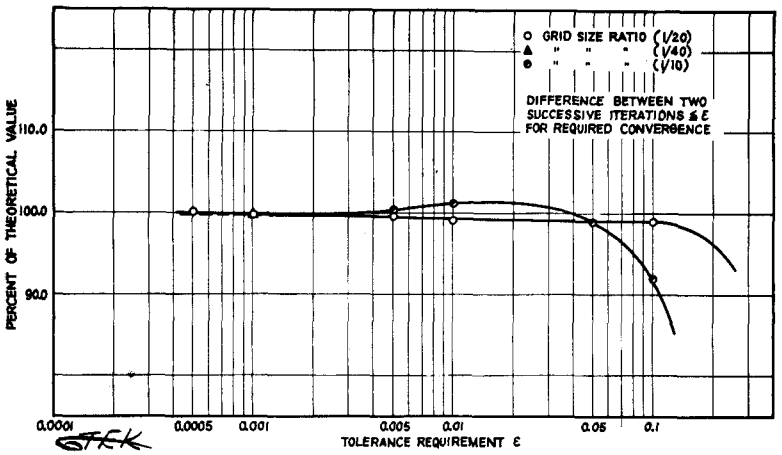

Fig. 12. The effect of grid size and tolerance requirement on the ratio of computed and theoretical values.

Figure 6 represents the cross-sectional area of pipe and its geometric boundaries as approximated by the indicated grid points. The black dots represent the boundary points where the fluid velocity w must equal zero. The interior points are denoted by white circles. The velocity field is computed on the Datatron by this relaxation routine, the results being given in Figure 7, where the circular points represent calculated velocities plotted against the background of theoretical parabolic velocity profile.

A large amount of practical information is obtained by starting the calculations on coarse grids and then repeating these calculations on smaller and smaller grids on specific cross-sectional areas of interest. The regions denoted as I, II, and III in Figure 6 indicate the subregions computed on smaller grid sizes.

Steady State Pressure Distribution in an Oil Reservoir

In an undersaturated reservoir the flow of oil in the steady state is usually governed by an elliptic partial differential equation

$$\nabla^2 P = 0 \qquad (10)$$

$$\frac{\partial^2 P}{\partial x^2} + \frac{\partial^2 P}{\partial y^2} = 0 \qquad (11)$$

The assumed boundary conditions are $P = 4{,}000$ at boundaries, $P_i = 1{,}000$ at $i = 1, 2, 3, 4, 5$ (producing wells). A circular reservoir as indicated in Figure 8 is considered with a five-spot group of wells producing at a constant bottom hole pressure. For this particular reservoir it is further assumed that the pressure is constant at the reservoir boundaries.

The steady state pressure distribution over the entire reservoir (approximated by the network as indicated) is calculated on the Datatron in approximately 12 min. The geometric location of wells, reservoir boundaries, and several computed isobars are given in Figures 8 and 9.

Heat Transfer in a Tubular Reactor

Steady state heat transfer calculations have been performed by using the developed relaxation routine to determine temperature distributions through the walls and within the packed interior of an internally finned vertical tubular reactor. Figure 10 represents the boundary geometry and the approximating network used on this problem and its conformal analogue. Only one half of the first quadrant is used owing to considerations of the inherent polar symmetry. For the first part of the problem, steady state, two-dimensional temperature distribution across the pipe walls, the differential equation is

$$\nabla^2 T = 0 \qquad (12)$$

To calculate the temperature distribution through the packed catalyst bed owing to heat dissipation throughout the inside volume the following equation is used:

$$\frac{\partial^2 T}{\partial x^2} + \frac{\partial^2 T}{\partial y^2} = -fT - g \qquad (13)$$

A square grid is used for this computation. The finite-difference equation used in this solution is given earlier as Equation 4*a*. Figure 11 represents the isotherms and heat-flow lines plotted after the results of relaxation calculations are performed on the computer.

Conformal Mapping

In solving the temperature-distribution problem through the pipe walls it became quite apparent that appreciably better representation of the geometric boundaries could be effected by performing the rectangular relaxation calculations on the conformal transform of the polar model. As indicated in Figure 10 the conformal transformation of the polar model by equations

$$\left.\begin{aligned} u &= \ln r \\ v &= \theta \end{aligned}\right\} \qquad (14)$$

results in a rectangular transform in the u, v, coordinate system. The model on the u, v plane is computed by the developed digitized relaxation routine, and the final temperature-distribution results are plotted on the actual model by using the transformation Equations (14).

Discussion of the Results and Conclusions

The digital relaxation routine developed for the Datatron is found to be effective fast, and practical in solving several steady state heat and mass transfer problems with arbitrary boundary conditions. In several cited examples the over-all computing speed is found to be about 250 iterations/min.

The computational accuracy achieved in these applications is studied in calculating several cases for which theoretically correct answers are available. This study indicates that the accuracy achieved during these computations is a function of both the grid size and tolerance specification incorporated in the routine. The effect of these two variables on the ratio of computed to theoretically known quantities is indicated in Figure 12. The tolerance requirement in this chart is a predetermined small number compared with the difference between two successive computed values at a given point. If the difference is equal to,

TABLE 1. SUMMARY ON TIME, GRID SIZE, AND TOLERANCES USED ON DIFFERENT PROBLEMS

Type of problem	Pressure distribution		Pipe flow		Heat transfer across reactor tube		Heat transfer across catalyst bed	
Elliptic equation solved	Laplace		Poisson		Laplace		Equation (7)	
Number of grid points	97	97	45	45	96	96	56	56
Tolerance requirement $u_n - u_{n-1}$	10 lb./ sq. in.	0.5 lb./ sq. in.	.1 ft./sec.	0.005 ft./sec.	0.1 °F.	0.01 °F.	0.1 °F.	0.01 °F.
Maximum value of dependent variable	4,000 lb./ sq. in.	4,000 lb./ sq. in.	50 ft./sec.	50 ft./sec.	1,172 °F.	1,172 °F.	1,135 °F.	1,135 °F.
Number of iterations	20	47	47	156	9	33	24	91
Total time, min.	6.5	15.2	7.5	26	2.3	8.9	3.7	14.1
Time/point, min.	0.07	0.16	0.16	0.57	0.02	0.09	0.07	0.25

or smaller than, (ϵ), the convergence at that point is considered satisfactory.

The data obtained from theoretically known laminar pipe-flow velocity-distribution calculations indicate that for a given grid size the computational accuracy increases with decreasing magnitude of tolerance requirement. As the tolerance becomes equal to, or smaller than, 0.05, the computation predicts the theoretical value approximately within 1%.

For tolerances less than 0.05 the computational accuracy also appears to be less affected by the grid size. In cases relating to extremely small grid sizes (that is, 40 or more increments per major geometric dimension), however, there are not enough data available to permit evaluating the effect of tolerance requirements.

The availability of as many as 1,000 interior and 800 boundary points, the average computational speed and accuracy proved in several case studies, indicate that this method is practical and useful in a large number of one- or two-dimensional steady state problems satisfying general Laplace-type differential equations. In addition, problems satisfying equations of the type of Equation (4) can also be solved by this digital technique.

The apparent rate of convergence is much faster in Laplace's equation than in Poisson's, or Equation (4). This is consistently observed in all calculated cases. Decreasing the tolerance scarcely affects the approximate results of the Laplace equations, but the approximate results of the Poisson-type equations are affected more drastically. Therefore one should be very careful in solving boundary-value problems satisfying Poisson's equation, since the fact that two consecutive iterations at each point differ by a very small quantity (ϵ) does not necessarily mean that the unknown function is as close as (ϵ) to its true value. The proved case studies in pipe-flow calculation however should give a fair indication of the nature of accuracy expected in solving the Poisson type of equation by this routine.

Table 1 summarizes the number of grid points used, tolerance requirements, the number of iterations, and time requirements on several types of problems solved.

ACKNOWLEDGMENT

The authors wish to acknowledge many helpful suggestions, assistance, and encouragement given by Don Tabler and several others during many phases of this study. Figures 10 and 11 have been included by permission of Tabler, who prepared the plots in connection with another engineering study. The constructive criticism and suggestions by L. W. Pollock resulted in several editorial improvements.

The authors also wish to thank the management of Phillips Petroleum Company for permission to present and publish this paper.

NOTATION

a = function of x and y
D/D_t = substantial time derivative
F_z = extraneous body force per unit mass
f = constant
g = constant
$g(x, y)$ = function of x and y variables
h = increment on a square grid
i = subscript
j = superscript or a subscript
n = interger representing the number of grid points considered
P = pressure, a dependent variable
r = radius, a polar coordinate
T = temperature, a dependent variable
u = dependent variable, function of x and y
w = velocity function in pipe flow
x = independent space variable
y = independent space variable
z = independent space variable
$\partial/\partial x$ = partial differentiation
∇^2 = Laplacian in Cartesian coordinates $\nabla^2 \equiv \partial^2/\partial x^2 + \partial^2/\partial y^2 \partial^2/\partial z^2$
Δ = finite difference, or increment
ρ = mass density
μ = viscosity
$\sum$ = summation
θ = divergence of the velocity vector
ϵ = tolerance requirement on dependent variable

LITERATURE CITED

1. Hartree, D. R., "Numerical Analysis," Oxford University Press (1955).
2. Scarborough, J. B., "Numerical Mathematical Analysis," 3 ed., The Johns Hopkins Press, Baltimore (1955).
3. Richardson, L. F., *Trans. Roy. Soc.*, **A, 210**, p. 307 (1910).
4. Liebmann, H., *Sitzber. math. physik, Kl. bayer. Akad. Wiss. Munchen*, 385 (1918).
5. Thom, A., *Aero Res. Comm. Rep. and Mem.*, No. 1194, 1928.
6. Shortley, G. H., and R. Weller, *J. Appl. Phys.*, 9 (May, 1938).
7. Southwell, R. V., "Relaxation Methods in Engineering Science," 1 ed., Oxford at the Clarendon Press (1946).
8. Southwell, R. V., "Relaxation Methods in Theoretical Physics," Oxford at the Clarendon Press (1949).
9. Shaw, F. S., "An Introduction to Relaxation Methods," Dover Publications, New York (1953).
10. Dykstra, H., and R. L. Parsons, *Trans. Am. Inst. Metall. Engrs.*, **192**, 227 (1951).

Manuscript received December 3, 1957; revision received February 12, 1958; paper accepted February 20, 1958; Paper presented at A.I.Ch.E. Chicago meeting.

Kinetics of the Thermal Decomposition of Calcium Carbonate

CHARLES N. SATTERFIELD and FRANK FEAKES

Massachusetts Institute of Technology, Cambridge, Massachusetts

There is considerable indication that the decomposition of calcium carbonate in the shape of, say, a sphere takes place essentially in the following manner. The reaction starts at the outside surface and proceeds towards the center in a relatively thin spherical reaction zone (Figure 1). At a given instant the center core is undecomposed calcium carbonate and the outer shell calcium oxide. The observed reaction rate is presumably determined by the interrelationships between three major rate processes:

1. *Heat Transfer.* Heat must first be transferred to the surface of the mass and then through the outer layer of calcium oxide to the reaction zone.

2. *Mass Transfer.* The carbon dioxide released at the reaction zone must escape through the outer shell of calcium oxide. Consequently, at finite rates of decomposition the pressure at the reaction zone must be greater than that at the surface of the sphere. The increase in pressure requires an increase in the temperature of the reaction zone to maintain decomposition. This in turn decreases the temperature difference causing heat transfer and consequently decreases the rate of reaction.

3. *Chemical Reaction.* The question here is whether any process associated with the decomposition reaction itself can be an over-all rate-limiting factor, for example whether the rate of nucleation or the nature of the interfacial surface at the reaction zone can affect the over-all rate of decomposition.

A considerable number of studies of calcination of calcium carbonate have been reported (*3, 5, 21, 22*), but the experimental results have usually been